Marine and Coastal Fisheries: Dynamics, Management, and Ecosystem Science 13:583–599, 2021

ISSN: 1942-5120 online
DOI: 10.1002/mcf2.10176

ARTICLE

The Relative Influence of Age Structure, Predation, and Temperature on Stock–Recruitment Dynamics: A Case Study of Southern New England/Mid-Atlantic Winter Flounder

Matthew R. Siskey*
School of Aquatic and Fishery Sciences, University of Washington, 1122 Northeast Boat Street, Seattle, Washington 98195, USA; and School of Marine and Atmospheric Sciences, Stony Brook University, 100 Nicolls Road, Stony Brook, New York 11794, USA

Michael G. Frisk
School of Marine and Atmospheric Sciences, Stony Brook University, 100 Nicolls Road, Stony Brook, New York 11794, USA

Abstract

Stock size estimates used in stock–recruitment models often assume that reproductive output per individual is equal despite evidence that larger, older spawners contribute diverse spawning behaviors and disproportionately more to reproductive output. This is concerning since depleted population states often coincide with a compromised age structure and increased control of extrinsic forces (environmental conditions or predator–prey dynamics) on stock productivity. In this study, parameterizations of the stock–recruitment relationship for Winter Flounder *Pseudopleuronectes americanus*, which incorporated covariate metrics describing age structure, temperature, and predation, were compared to identify primary drivers across area-specific data sets that are included in recent regional stock assessments. Four of the six data sets resulted in a top-ranked model that incorporated an age structure metric; however, the age structure metric model was alone in the pool of top-ranked models for only two of these scenarios. In addition, one data set resulted in a base Ricker model, and one resulted in a model that incorporated a predator index. Finally, wavelet analysis identified significant coherence between fishing mortality rate (*F*) and spawning stock biomass (SSB) for Winter Flounder, which switched from an out-of-phase state to an in-phase state during the 1990s. If the relationship between these model-derived estimates of *F* and SSB reflects dynamics of the Winter Flounder population, it would have strong implications for management efforts.

Understanding the relative role of biological, abiotic, and stochastic drivers of the stock–recruitment (SR) relationship remains a fundamental challenge in fisheries science. Regardless of the functional form used (i.e., Ricker or Beverton–Holt [BH]), the SR relationship is rooted in the basic idea that the abundance of a new cohort entering the population is, to some extent, a function of adult abundance (Hilborn and Walters 1992; Quinn and Deriso 1999). Stock–recruitment relationships are represented by a variety of functional forms that involve density-dependent dynamics; however, units of adult abundance or biomass are often assumed to be equal

*Corresponding author: msiskey@uw.edu
Received October 14, 2020; accepted June 26, 2021

despite evidence that larger, older spawners contribute diverse spawning behaviors (Hixon et al. 2014) and disproportionately more to fecundity and total reproductive output (Barneche et al. 2018). Moreover, basic forms of the SR relationship assume that external forces (e.g., temperature, predation, and fishing) act similarly on a stock regardless of its demographic state (e.g., distribution of size- or age-classes).

Size-selective fishing is known to cause demographic changes to fish populations, resulting in a diminished age structure (i.e., age truncation), changes in life history parameters (e.g., size at age, size at maturity, or age at maturity), and shifts to low-abundance population states (Harris and McGovern 1997; Hutchings 2000; Durant et al. 2013; Vert-pre et al. 2013; Siskey et al. 2016; Kerr et al. 2017). A truncated age structure can compromise the efficacy of the storage effect, which describes the capacity of an intact age structure to buffer a population from periods of unfavorable environmental conditions. Here, an intact age structure facilitates the persistence of a population or stock through repeated spawning across years that are characterized by variable spawning and nursery conditions (Elmqvist et al. 2003; Secor 2007). In addition, older spawners tend to spawn at different times of the spawning season and at different locations on the spawning grounds than younger adults (Hixon et al. 2014; Secor 2015). Thus, a population that is heavily reliant on first-time female spawners ("recruit spawners"), which are usually smaller and produce fewer eggs, is likely to produce weaker year-classes based on overall reproductive energy output (Barneche et al. 2018). Furthermore, in population states that are characterized by depleted abundance and a compromised age structure, the variability of recruitment and population abundance has been found to increase in frequency (e.g., a change from low frequency variability to low and high frequency variability) and more closely track environmental variability (Hsieh et al. 2006; Rouyer et al. 2011, 2012). Since a truncated age structure negatively affects recruitment, the stability of population dynamics, and population persistence, it is pertinent to consider this factor in the SR relationship and potential recovery efforts (Anderson et al. 2008; Rouyer et al. 2012; Hixon et al. 2014).

In the case of southern New England/mid-Atlantic (SNE/MA) Winter Flounder *Pseudopleuronectes americanus*, adult abundance and recruitment have declined precipitously over the exploitation history of the stock, associated with chronic and selective overexploitation (fully selected fishing mortality rate of 0.80–1.08 from 1985 to 1993; NEFSC 2017a). Despite reductions in fishing mortality rate (F), low adult abundance and low recruitment have persisted since the stock collapsed in the 1990s, suggestive of a regime shift to a low-production state and a lack of control on spawning stock biomass (SSB) through alterations to fishing mortality. Climate change has been suggested as a major impediment to recruitment and overall recovery of the stock (Bell et al. 2015, 2018); however, it is also important to consider any historical demographic changes that overfishing has imposed on the population, which may have preconditioned it for collapse or modified its ability to recover in suboptimal climatic conditions (Perry et al. 2010; Planque et al. 2010). If this is the case, then strict management measures focused on recovering age structure could have a positive influence on recovery and bolster the population against future, impending changes to the climate. Recovery in age structure could generate a boost to recruitment; however, it may take time periods analogous to a generation or more in order for the population to realize the potential of a fully intact age structure on recruitment success.

In addition to the direct effects imposed by climate change on a cold-adapted species such as the Winter Flounder (e.g., thermal stress via warmer winter temperature and earlier spring warming), climate change has also induced range expansions for several known predators of Winter Flounder in the region, which has the potential to increase residence time and habitat overlap of predatory species with young-of-the-year (age-0) Winter Flounder on nursery grounds (e.g., Summer Flounder *Paralichthys dentatus*; Nye et al. 2009; Pinsky and Fogarty 2012; Bell et al. 2015). This can have an indirect effect on survival of age-0 Winter Flounder in their first summer (Frisk et al. 2018), which should be considered in SR analyses. Identifying the relative influence of these recruitment drivers has an added utility in that accounting for additional sources of variation will allow for better forecasting. In turn, this could potentially benefit management of the stock since recommendations for future catches are typically based on forecasts that incorporate recruitment.

Drivers of the SR relationship (i.e., age structure, climate, and predation) may also vary across spatial units (e.g., different spawning or nursery environments within a regional stock unit) or spatial scales (i.e., individual versus aggregated nurseries). This is especially true for Winter Flounder, as evidence of complex population structure (e.g., ocean and inshore substocks; partial migration) exists across both the SNE/MA and Gulf of Maine coastal stock units based on acoustic telemetry (DeCelles and Cadrin 2010; Sagarese and Frisk 2011; Fairchild et al. 2013; Ziegler et al. 2018), otolith chemistry (Siskey et al. 2020), and fisheries surveys (Wuenschel et al. 2009; Fairchild 2017). If state-specific estuarine systems and oceanic subregions within the regional stock unit are reproductively isolated, then the dominant drivers of the SR relationship may vary based on geographic differences in abiotic conditions (i.e., temperature or predatory stress).

In addition, SR drivers may differentially affect survival across stages of early life history (e.g., larval, settlement, or juvenile periods), with previous work focusing on the egg and larval stages (Jeffries and Johnson 1974; Jeffries and Terceiro 1985; Keller and Klein-MacPhee 2000; Taylor and Collie 2003). Data available for the SNE/MA Winter Flounder stock assessment include age-1 data from the ocean environment and age-0 data from inshore coastal bay nursery habitats. Using both of these data sets, Frisk et al. (2018) found that recruitment trends and overall productivity have differed markedly between inshore coastal bay (age-0) and ocean (age-1) surveys, with recruitment increasing in estuaries but decreasing in ocean surveys. This analysis indicated a compensatory response in recruitment during the 2000s. These findings help to refine hypotheses for the recruitment failure in Winter Flounder and highlight the need to understand the influence of stock structure definitions (i.e., spatial scale) and recruitment drivers when parameterizing the SR function. Thus, a formal analysis considering spatially specific recruitment patterns as well as the full suite of recruitment drivers is necessary to comprehensively assess Winter Flounder SR dynamics, identify which mechanisms influence stock productivity and recruitment success, and determine whether these mechanisms differ across spatially explicit spawning and nursery habitats of the regional stock unit.

In this study, we first developed age structure metrics that captured the range and diversity of ages across various population states. These metrics, along with climate and predator abundance metrics, were used to evaluate covariate parameterizations of the SR relationship in order to identify any influence they have had on spawner–recruit relationships. This analysis was conducted using six different SR data sets from the various subregions of the regional SNE/MA stock unit to identify which recruitment drivers are most influential across spatial components of the stock. Specifically, we evaluate recruitment drivers representing (1) the breadth of age-classes within the spawning stock (number of spawner age-classes [ACs]), (2) the proportion of those age-classes that are first-time spawners (recruit spawners [% RS]), (3) the abundance of a common predator (Summer Flounder), and (4) bottom temperature (BT). Finally, we used time series analysis to identify coherency between model-derived F and SSB outputs across the exploitation history of the stock. This allowed us to track the relationship of the two metrics, which are critical for successful management controls.

METHODS

Data and metrics.— Data available for this study included stock and recruitment indices of abundance at age for the SNE/MA ocean shelf region taken from the National Marine Fisheries Service (NMFS) Bottom Trawl Survey (BTS; ocean spring and ocean fall) as well as stock and recruitment indices for inshore estuarine systems within the SNE/MA region taken from state surveys (Table 1). These data were obtained from the model input data file for the 2017 SNE/MA stock assessment (NEFSC 2017a), which includes both state and federal survey indices of abundance at age. Model files are publicly available via the Northeast Fisheries Science Center's Stock Assessment Support Information portal (https://apps-nefsc.fisheries.noaa.gov/saw/sasi/sasi_report_options.php). Since the data obtained were already age specific, no conversion of length data to age data was conducted. However, to provide some context, a design-based estimator is used by state and federal scientists in order to provide the indices of abundance at age and age composition information to the stock assessment team for use in the model. In this case, this involves weighting average numbers per tow (CPUE) by stratum size (area) and converting stratified mean numbers per tow at length to stratified mean numbers per tow at age by using an age–length key (i.e., conditional age at length). In addition, since these data are used as model input, the data products have already been adjusted for the vessel change that occurred for the NMFS-BTS in 2009 based on extensive calibration

TABLE 1. List of surveys and associated data types used in stock–recruitment models for Winter Flounder (CT-DEEP = Connecticut Department of Energy and Environmental Protection; RI-DEM = Rhode Island Department of Environmental Management; MA-DMF = Massachusetts Division of Marine Fisheries; NMFS-BTS = National Marine Fisheries Service Bottom Trawl Survey).

Agency	System	Data	Area
CT-DEEP	Long Island Sound	Stock (age 3+), recruitment (age 0), Summer Flounder (age 1+), bottom temperature	Inshore
RI-DEM	Narragansett Bay	Stock (age 3+), recruitment (age 0), Summer Flounder (age 1+), bottom temperature	Inshore
MA-DMF	Buzzards Bay	Stock (age 3+), recruitment (age 0), Summer Flounder (age 1+), bottom temperature	Inshore
NMFS-BTS	Ocean	Stock (age 3+), recruitment (age 1), Summer Flounder (age 1+), bottom temperature	Ocean

studies. Therefore, no further correction of data products used in this study for a vessel effect was necessary. Please see the most recent benchmark stock assessment for SNE/MA Winter Flounder and references therein for information on these vessel calibration studies and how survey data products were adjusted accordingly (NEFSC 2011).

For federal surveys, ocean spring and ocean fall data sets were used separately (not combined) in comparisons as outlined below. For state surveys, spring trawl survey data were used whereby "-at-age" data were stratified so that data for age-3 and older (age-3+) fish were used to construct the "stock" indices. Ocean stock data included mean number of age-$3+_{t-1}$ individuals per tow, while ocean recruit data included mean number of age-1_t individuals per tow. Inshore stock data (mean number of age-$3+_{t-1}$ fish per tow) were obtained from the Connecticut Department of Energy and Environmental Protection's (CT-DEEP) Long Island Sound Trawl Survey, the Massachusetts Division of Marine Fisheries' (MA-DMF) Inshore Trawl Survey, and the Rhode Island Department of Environmental Management's (RI-DEM) Coastal Trawl Survey. Inshore recruit data (mean number of age-0_t fish per tow) were obtained from the MA-DMF Estuarine Seine Survey, the RI-DEM Narragansett Bay Seine Survey, and the CT-DEEP Seine Survey.

In addition to being used separately, the stock and recruitment indices of abundance from state surveys were subsequently corrected for area swept differences across surveys and were aggregated to develop a regional inshore data set that complemented the two season-specific, regional ocean data sets used in stock assessment (NMFS-BTS ocean fall and ocean spring). This was conducted by first expanding each separate state survey's index at age annually for the area swept, then summing across ages within each survey, and finally taking the average of area swept-corrected indices across state surveys annually. The surveys that were combined to create the aggregated inshore adult index share a similar dome-shaped selectivity pattern whereby ages 3 and 4 are fully selected and selectivity subsequently diminishes with increasing age-classes (ages 5, 6, and 7+; NEFSC 2017a). These similar selectivity patterns suggest negligible effects of survey-specific selectivity biasing the aggregated index (i.e., due to different vessels or gears across surveys); therefore, no correction of the data was conducted to account for differences in selectivity. For information on survey gear and protocols, please see the most recent benchmark stock assessment report and various area-specific reports cited therein for respective state and federal survey protocols (NEFSC 2011).

Age structure, predation, and temperature data were compiled for inshore and ocean areas and converted to *z*-scores for use as covariates in the SR analysis before inclusion in any models (Hilborn and Walters 1992; Quinn and Deriso 1999). Age structure data were compiled from the NMFS otolith archive for Winter Flounder, which is the result of extensive sampling ($N = 20{,}112$) in the SNE/MA region for the period 1976–2018. These age data were otolith-derived age estimates, which are typically a product of multiple reads (i.e., "specimen" age data). The age data were not scaled up to the population level using size composition information (i.e., length frequency information expanded by CPUE and stratum area) and an age–length key to account for rare observations in marginal age-classes (ages 10+). A plus group that spans 50% of the SNE/MA Winter Flounder's age-classes (age 7+) is used for this stock, and there is considerable overlap in size at age in the oldest age-classes, suggesting a low probability of assigning larger individuals to the correct age-class. Therefore, it is likely that marginal age-classes are underrepresented in this study.

Due to the comprehensive nature of this sample and the lack of a complementary otolith archive for the inshore area, these age data were used in both inshore and ocean models. Despite the fact that the NMFS-BTS discontinued sampling of the most inshore ocean strata after a vessel change in 2008, we believe that it was appropriate to use these data to develop inshore SR covariate models. Coastal stocks of Winter Flounder have historically been categorized as obligate annual migrants, which move from inshore, estuarine spawning and nursery grounds where they spawn in the winter to ocean shelf foraging grounds in the summer (NEFSC 2011). However, as reviewed above, recent work has found potential substock structure and partial migration across the coastal stocks. According to these population structure definitions, approximately 70% of Winter Flounder ecotypes (bay migrants, ocean residents, and ocean migrants; Siskey et al. 2020) utilize the coastal ocean environment; thus, the NMFS-BTS otolith samples are representative of at least 70% of the regional unit.

Metrics developed to describe the age structure of the stock included the number of spawner ACs and % RS (i.e., first-time spawners). These two metrics were used to represent the breadth of the age structure of the spawning stock (ACs) and the proportion of the spawning stock that is composed of recruit spawners (% RS), respectively. "Spawners" were defined as age-3+ individuals according to the accepted maturity ogive reported in the stock assessment (NEFSC 2017a), which estimates 56% maturity at age 3 and 95% maturity at age 4. We calculated % RS using the equation

$$\%\ \mathrm{RS} = \frac{\text{Count of age} - 3 \text{ individuals}}{\text{Count of age} - 3 \text{ or older individuals}}.$$

Annual ocean BT anomalies were taken from the Northeast Fisheries Science Center's *State of the Ecosystem* report for the Middle Atlantic Bight region (NEFSC 2020) for the years 1981–2018. Annual BT data for the three major estuaries in the SNE/MA region were constructed from MA-

DMF (Buzzards Bay), CT-DEEP (Long Island Sound), and University of Rhode Island–Graduation School of Oceanography (Narragansett Bay, Fox Island Station) state surveys for the years 1981–2018 (Table 1). The MA-DMF survey collects data in the spring (May) and fall (September). The CT-DEEP survey collects data in April, May, June, September, and October. The University of Rhode Island–Graduation School of Oceanography survey collects data during every month. For each of these data sources, annual mean temperature data were constructed by taking the mean for each year, and z-scores were then calculated for each data set separately. In addition to being used separately for state-specific SR analyses, the three inshore temperature time series were averaged prior to being converted to annual z-scores to generate one temperature index that covered the range of time for which Winter Flounder stock and recruitment data were available (1981–2016).

An ocean predation index was compiled for Summer Flounder, which is an important predator of age-0 Winter Flounder according to field and laboratory experiments (Manderson et al. 2000; Sagarese et al. 2011), suggesting that the population sizes and overlapping summer residency of Summer Flounder with age-0 Winter Flounder nurseries could impact age-0 Winter Flounder survival. Summer Flounder (ages 1–10) data for the ocean shelf area were taken from NMFS-BTS fall and spring surveys, while the estuarine Summer Flounder predation index was compiled from the MA-DMF spring survey (ages 1–8+), the RI-DEM fall survey (ages 0–9+), and the CT-DEEP spring survey (ages 1–7+). In addition to being used separately in state-specific SR analyses, the three predator indices were corrected for area swept differences across surveys, averaged, and converted to annual z-scores to generate an aggregated inshore predator index that spanned the range of time for which Winter Flounder stock and recruitment data were available (1981–2016). Other predators were considered for use in the predation index (e.g., Striped Bass *Morone saxatilis*, Bluefish *Pomatomus saltatrix*, and blue crab *Callinectes sapidus*), but Summer Flounder was the only predator species for which data were available comprehensively across all systems and years of interest in parallel to Winter Flounder data.

Stock–recruitment analyses.— A model selection exercise was conducted to compare the relative fit of base Ricker (1954) and base BH (Beverton and Holt 1957) SR models to covariate parameterizations of these models (i.e., fit to spawner [age $3+_{t-1}$], recruit [age 0_t or age 1_t], as well as age structure, temperature, or predation covariate data; Hilborn and Walters 1992; Quinn and Deriso 1999). Models were fitted separately to each data set by geographic area to understand the potential drivers of the SR relationship spatially, as major estuaries likely represent production units, partially owing to the existence of natal homing in this species (Phelan 1992). In addition, previous work that investigated the genetic diversity of breeders across estuarine systems in the study area found a high level of potential inbreeding within estuarine systems and evidence of local population structure (O'Leary et al. 2013). The authors attributed this finding to the highly depleted nature of the population and the existence of natal homing, which may have facilitated the concentrated spawning groups within these systems.

Covariate SR models and base SR models were compared in this analysis. The covariate model structure incorporated a covariate coefficient (γ) for the effects of the covariate X (Hilborn and Walters 1992). The covariate BH model structure was

$$R_t = \frac{\alpha S_{t-1}}{\beta + S_{t-1}} e^{\gamma(X_{t-1})+\varepsilon},$$

and the covariate Ricker model structure was

$$R_t = S_{t-1} e^{\alpha - \beta S_{t-1} + \gamma(X_{t-1})+\varepsilon},$$

where R is the abundance of recruits, S is the stock size, X is the covariate data, α is the density-independent term, β is the density-dependent coefficient, and γ is the coefficient for the effect of X. Here, covariate z-scores for % RS, BT, and Summer Flounder indices were inverted (i.e., the sign was changed) such that in all covariate z-score data sets, positive values were considered better for Winter Flounder recruitment (e.g., lower % RS, lower BTs, and lower Summer Flounder abundance). Covariate models only included a single covariate, so model comparisons were only across single-covariate models.

Models were fitted in log space with maximum likelihood assuming lognormal errors, and model selection was conducted using Akaike's information criterion (AIC; Burnham and Anderson 2002). To evaluate the potential drivers of recruitment, all covariates and related model structures were given equal a priori weights.

We estimated AIC weights (w_i) for all models as

$$w_i = \frac{e^{-\frac{1}{2}\Delta_i(\mathrm{AIC})}}{\sum_{k=1}^{K} e^{-\frac{1}{2}\Delta_k(\mathrm{AIC})}},$$

where Δ_i(AIC) is the difference of the AIC between the top-ranked model and each candidate model and K is the total number of models compared. Evidence ratios (ERs) were also calculated to provide a measure of the improvement in model predictive ability between the top-ranked model and each of the other candidate models,

$$\mathrm{ER} = \frac{w_{R_1}(\mathrm{AIC})}{w_{R_i}(\mathrm{AIC})},$$

where R_1 is the top-ranked model and R_i are each of the other candidate models. Finally, predicted versus observed recruitment and the residuals from this relationship relative to predicted recruitment are reported in the Appendix in order to demonstrate goodness of fit and improvements in these metrics across the top-ranked models. The slope of predicted versus observed recruitment and the adjusted r^2 value of this relationship are also reported in the Appendix.

Fishing mortality and stock size.—The relationship between F and SSB time series generated from the SNE/MA regional stock assessment was explored using spectral analysis to identify coherence between these time series and the frequency at which they cohered. Wavelet coherence provides a measure of the coherence of oscillations for nonstationary signals (Cazelles 2008; Rouyer et al. 2012). In other words, it is a measure of the correlation between the two time series estimated by the stock assessment (F and SSB). Here, wavelet power spectra and coherence of the time series in the time/frequency domain were calculated using the WaveletComp package in R, with cross-wavelet power spectra computed using Morlet wavelets (R Core Team 2018; Roesch and Schmidbauer 2018). Statistical significance of the coherence between the two time series was assessed using a simulation algorithm, which is a feature of the WaveletComp package ($N = 100$ simulations). This analysis was conducted to provide a view into the nature of coherence between SSB and F over the time period of interest, whereby high coherence suggests that SSB and F are influencing each other, while low coherence suggests a decoupling of these variables. This analysis was conducted to provide an evaluation of how the assessment is tracking these two metrics. If they are not linked, it could suggest that other mechanisms not specifically modeled in the assessment are driving the stock's dynamics (e.g., temperature, predation, and age structure). Here, an out-of-phase state is when F and SSB deviate in opposite directions, and an in-phase state is when they deviate in the same directions.

There has been criticism over the use of model output as "data," and rightfully so (Brooks and Deroba 2015). In particular, a point has been made that there is inherent correlation among model outputs (e.g., F and SSB), which are related when fitting stock assessment models. Therefore, in this study F and SSB model outputs from the SNE/MA Winter Flounder assessment were used to identify whether a correlation did exist and whether it persisted throughout the assessment history (i.e., whether F retained management control of SSB) or was lost at some point. Since 2008, the SNE/MA Winter Flounder stock assessment has employed a split structure at 1993/1994, which has allowed potential changes in fishery and biological parameters in the mid-1990s to be captured (NEFSC 2011). As a result, the retrospective pattern that had been categorized as extreme prior to 2008 is now reported as minor (NEFSC 2017a), so no retrospective adjustments were conducted on the model output used herein. Furthermore, as seen below, identified changes in the relationship between F and SSB do not occur at this split, suggesting that the split structure did not affect F and SSB output to an extent that would influence the wavelet coherence analysis.

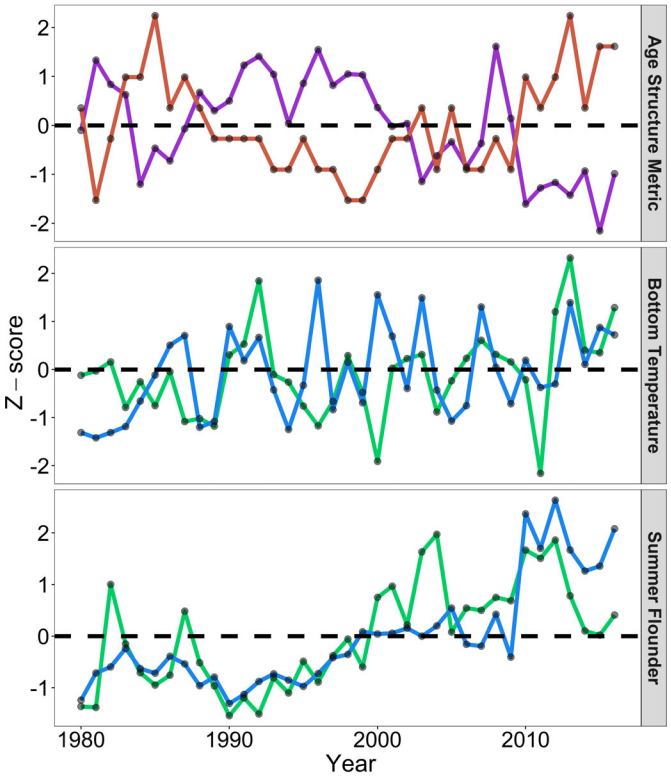

FIGURE 1. The z-scores of age structure metrics for Winter Flounder over time (top panel): number of spawner age-classes (orange) and percentage of recruit spawners (purple). Bottom temperature (middle panel) and Summer Flounder (bottom panel) z-scores over time periods of the stock–recruitment analysis are depicted for inshore (green) and ocean (blue) areas. The z-scores shown were not inverted.

RESULTS

Age Structure, Climate, and Predation Metrics

Some general trends in age structure metric z-scores were apparent over time (Figure 1, top panel). In the first half of the time series (1980–2000), there was a decline in spawner ACs and a corresponding increase in % RS, suggesting a reduction in spawner age structure (e.g., age truncation, or reduced number of spawner ACs). In the second half of the time series (2000–2016), ACs increased back to positive anomalies and % RS returned to negative levels, suggesting recovery of the age structure.

Bottom temperature underwent fewer systematic fluctuations across the time series compared to age structure, with frequent oscillations between positive and negative values (Figure 1, middle panel). Inshore and ocean BT anomalies followed similar trends in the 1980s and early 1990s, with mostly negative BT anomalies in the 1980s. In the late 1990s and early 2000s, BT anomalies oscillated between positive and negative values much more frequently, with inshore and ocean temperature anomalies deviating in opposite directions in some years (ocean positive, inshore negative). From the late 2000s through the remainder of the time series, both data sets fluctuated in general synchrony. In the last 4 years of the time series (2012–2016), both inshore and ocean BTs were positive.

The anomalies for the Summer Flounder predation metric were very similar across regions (Figure 1, bottom panel). In the first half of the time series (1980–2000), both inshore and oceanic Summer Flounder indices were negative except for two inshore years with positive Summer Flounder values. From 2000 to 2016, the Summer Flounder indices shifted to almost entirely positive values, with the only three negative values occurring in the ocean index from 2006 to 2009.

Working with covariate z-scores as included in SR models below (SF, BT, and % RS z-scores reversed, so bigger is better), Spearman's rank correlations were calculated between each covariate within each data set (i.e., ocean fall, ocean spring, aggregated inshore, MA-DMF, CT-DEEP, and RI-DEM). This correlation analysis was conducted to ensure that there were no extreme correlations across covariates, which would suggest that exclusion was appropriate. The correlation between age structure metrics was positive and ranged from 0.61 to 0.64 in magnitude across the different spatial units. The BT covariate was only correlated with another covariate in the MA-DMF data set, where it was negatively correlated with % RS (−0.52). The Summer Flounder covariate was only correlated with another covariate in the ocean spring and CT-DEEP data sets. In the ocean spring data set, the Summer Flounder covariate was negatively correlated with % RS (−0.54). In the CT-DEEP data set, it was negatively correlated with % RS (−0.66) while also being negatively correlated with the number of spawner ACs (−0.54).

Stock–Recruitment Analyses

Using the SR data from the NMFS-BTS, the top-ranked models differed between the ocean spring and ocean fall data sets (Table 2; Figure 2). Models were compared and deemed different via ΔAIC greater than 2 and separation of ERs greater than 2 (Burnham and Anderson 2002), where ERs are the ratio of w_i between models compared (i.e., the weight of relative evidence compared across models). In addition, goodness of fit was examined across the top-five ranked models using comparisons between predicted and observed recruitment (Appendix Table A.1; Appendix Figure A.1) and residual versus predicted recruitment relationships (Figure A.2). The top-ranked model using the ocean spring data was the BH model that incorporated Summer Flounder as a covariate (SF BH). This model estimated a negative β, suggesting higher survival rates with increasing stock size. Across the top-five ranked models, one can observe a transition from no relationship between predicted and observed recruitment to a stronger one (Table A.1; slope = 0.012 in the ACs BH model to 0.128 in the SF BH model), as well as an increase in the adjusted r^2 value in this relationship (adjusted $r^2 = -0.023$ in ACs BH model to 0.113–0.164 in the top-two ranked models, which were very similar with reference to AIC). The top-two models using the ocean fall data both incorporated the number of spawner ACs as a covariate (ACs Ricker and ACs BH models). Compared to the base models, the top models for these data sets predicted more variable recruitment at medium to high stock sizes. There was also an increase in the adjusted r^2 value for the relationship between predicted and observed recruitment across the top-five ranked models (adjusted $r^2 = 0.109$–0.193). One can also observe some improvement in model fit from the Ricker model (the fifth-ranked model), which shows a cone-shaped pattern in the residuals plot, to the top-ranked models, which have little to no pattern in the residuals (Figure A.2).

Using the SR data aggregated from the inshore state surveys, the top model did not include any covariates (Ricker; Table 2; Figure 2). The top-two ranked models (Ricker and BH) had the highest values of adjusted r^2 out of the top-five ranked models (Table A.1; adjusted $r^2 =$ 0.485–0.529). In addition, the top-ranked model (Ricker) was the only model without a pattern in the residuals plot (Figure A.2). Using the SR data from each separate state survey, there was only one top-ranked model for the CT-DEEP and RI-DEM data sets but three top-ranked models for the MA-DMF data set. With the MA-DMF data, the top-three models included the number of spawner ACs, BT, and % RS as covariates in a BH model. Here, compared to the base BH model, the ACs BH model predicted higher recruitment at low stock sizes and predicted lower recruitment at medium to high stock sizes. Across all of the top-five ranked models for the MA-DMF data set, none had a pattern in the residuals plot (Figure A.2), and all AIC and adjusted r^2 values were quite similar (Tables 2, A.1; adjusted $r^2 = 0.284$–0.339). With the CT-DEEP data, the top-ranked model included the number of spawner ACs as a covariate in a BH model (ACs BH; Table 2; Figure 2). Compared to the base BH model, this model predicted generally similar but more variable recruitment at low to medium stock sizes and predicted

TABLE 2. Difference in Akaike's information criterion (ΔAIC) values, evidence ratios (ERs), parameter estimates, and likelihood of models using each Winter Flounder data set (BH = Beverton–Holt; ACs = number of spawner age-classes; RS = percent recruit spawners; BT = bottom temperature; SF = Summer Flounder predation index). Agency acronyms are defined in Table 1; parameter symbols are defined in Methods.

Model	ΔAIC	ER	α	β	γ	ε	Log-likelihood
NMFS-BTS ocean spring							
SF BH	0.000	1.000	0.159	−0.179	0.437	−0.254	22.57
BT BH	2.980	4.436	0.184	−0.079	0.339	−0.214	21.08
RS BH	4.907	11.63	0.165	−0.144	−0.274	−0.188	20.11
BH	6.093	21.04	0.179	−0.068		−0.145	18.52
ACs BH	6.855	30.80	0.171	−0.109	−0.166	−0.161	19.14
BT Ricker	10.34	175.6	−1.105	0.461	0.376	−0.114	17.40
Ricker	13.46	838.3	−1.188	0.430		−0.045	14.84
SF Ricker	14.74	1,587	−1.125	0.478	0.140	−0.055	15.20
ACs Ricker	15.17	1,973	−1.190	0.426	−0.086	−0.049	14.98
RS Ricker	15.38	2,188	−1.176	0.439	−0.046	−0.046	14.88
NMFS-BTS ocean fall							
ACs Ricker	0.000	1.000	−0.539	0.404	−0.446	−0.102	−7.286
ACs BH	0.392	1.216	0.692	0.892	−0.470	−0.096	−7.482
SF Ricker	2.712	3.881	−0.566	0.425	−0.368	−0.062	−8.642
SF BH	4.072	7.660	0.719	1.140	−0.344	−0.042	−9.322
Ricker	5.180	13.33	−0.748	0.350		0.004	−10.88
BT Ricker	5.640	16.78	−0.764	0.318	0.246	−0.019	−10.11
BH	5.947	19.56	0.806	1.581		0.015	−11.26
BT BH	6.012	20.20	0.868	1.679	0.274	−0.013	−10.29
RS Ricker	6.799	29.96	−0.739	0.348	−0.107	−0.002	−10.69
RS BH	7.378	40.01	0.786	1.468	−0.133	0.007	−10.98
Inshore							
Ricker	0.000	1.000	5.171	1.290×10^{-4}		−1.063	−416.1
BH	68.20	6.444×10^{14}	2.118×10^{10}	1.260×10^{9}		0.163	−450.2
ACs BH	109.7	6.506×10^{23}	1.073×10^{4}	−503.6	−0.327	0.643	−470.0
SF BH	137.3	6.386×10^{29}	1.296×10^{8}	9.028×10^{7}	−0.360	1.017	−483.8
BT BH	144.2	2.078×10^{31}	2.253×10^{8}	2.199×10^{8}	0.308	1.106	−487.3
RS BH	159.8	5.152×10^{34}	835.5	−517.6	−0.462	1.305	−495.1
SF Ricker	281.1	1.119×10^{61}	34.32	0.008	18.96	2.928	−555.7
BT Ricker	322.2	9.418×10^{69}	60.52	0.013	0.559	3.508	−576.3
ACs Ricker	322.3	9.720×10^{69}	60.52	0.013	0.212	3.509	−576.3
RS Ricker	322.4	1.045×10^{70}	60.51	0.013	0.212	3.510	−576.4
MA-DMF							
ACs BH	0.000	1.000	0.684	4.511	0.123	−0.848	38.22
BT BH	0.042	1.021	0.806	6.831	−0.146	−0.848	38.20
RS BH	1.266	1.883	0.720	5.485	0.101	−0.830	37.59
SF BH	2.033	2.763	0.632	3.750	0.059	−0.819	37.21
BT Ricker	2.626	3.718	−2.601	0.041	−0.219	−0.811	36.91
ACs Ricker	3.795	6.669	−2.485	0.052	0.189	−0.796	36.33
RS Ricker	4.344	8.777	−2.574	0.046	0.182	−0.788	36.05
Ricker	7.146	35.627	−2.589	0.050		−0.707	33.65
BH	20.29	2.552×10^{4}	2.054	51.53		−0.518	27.08
SF Ricker	255.6	3.247×10^{55}	4.416	0.428	−14.15	2.721	−89.59
CT-DEEP							
ACs BH	0.000	1.000	4.355	4.942	−0.758	−0.167	−63.68
SF Ricker	2.310	3.174	−0.669	0.034	0.629	−0.129	−64.83
ACs Ricker	2.798	4.050	−0.999	0.027	−0.600	−0.109	−65.08

TABLE 2. Continued.

Model	ΔAIC	ER	α	β	γ	ε	Log-likelihood
SF BH	4.395	9.002	6.404	10.83	0.536	−0.089	−65.88
RS BH	4.414	9.090	3.726	1.829	−0.685	−0.088	−65.89
Ricker	9.564	119.4	−1.243	0.018		0.043	−69.46
BH	9.746	130.7	8.937	28.21		0.043	−69.55
BT Ricker	11.51	315.2	−1.275	0.018	0.051	0.048	−69.43
BT BH	11.62	332.8	9.150	29.48	0.076	0.040	−69.49
RS Ricker	212.0	1.101×10^{46}	58.02	1.779	−18.49	3.587	−169.69
			RI-DEM				
ACs BH	0.000	1.000	21.32	3.036	−0.267	−0.339	−101.2
BH	1.433	2.047	22.19	3.624		−0.284	−102.9
ACs Ricker	1.480	2.096	1.517	0.097	−0.240	−0.315	−101.9
Ricker	2.216	3.029	1.458	0.091		−0.272	−103.3
RS BH	2.684	3.826	20.39	2.811	−0.124	−0.295	−102.5
SF BH	3.201	4.956	21.44	3.271	0.067	−0.287	−102.8
BT BH	3.426	5.546	22.13	3.603	−0.011	−0.284	−102.9
RS Ricker	3.597	6.042	1.546	0.103	−0.116	−0.281	−103.0
SF Ricker	3.873	6.935	1.533	0.101	0.089	−0.276	−103.1
BT Ricker	4.180	8.085	1.470	0.094	−0.025	−0.273	−103.3

lower recruitment at higher stock sizes. The top-ranked model for the CT-DEEP data set had little to no pattern in the residuals plot relative to the other models included in the top-five ranked list. In addition, this model had the highest adjusted r^2 value (0.284). With the RI-DEM data, the top-ranked model included the number of spawner ACs as a covariate in a BH model (ACs BH; Table 2; Figure 2). Compared to the base BH model, the top-ranked model predicted similar but more variable recruitment across all stock sizes. None of the top-five ranked models had a pattern in the residuals plot, and there was an increase in the adjusted r^2 value across the list of top-five ranked models (adjusted $r^2 = 0.096$–0.115).

Fishing Mortality and Stock Size

The relationship between F and SSB began with a steep decline in SSB as F increased (Figure 3). Spectral analysis of regional estimates of SSB and F taken from NMFS stock assessment model output showed statistically significant coherence across 100 simulations between the time series from 1991 to 2016 (Figure 4, red area). This analysis also indicated that the time series transitioned from an out-of-phase state (SSB and F deviating in opposite directions) in the early 1990s to an in-phase state (SSB and F deviating in the same directions) by the late 1990s, remaining in this state for the duration (i.e., transition from arrows pointing up/left to arrows pointing up/right in Figure 4). This transition corresponded to a simultaneous shift from low-period/high-frequency fluctuations in the time series to high-period/low-frequency fluctuations (y-axis of plot), perhaps indicating a shift to a low-recruitment stable state. This represents a shift in the stock assessment output from a cycle approximately every 4 years to a cycle approximately every 8 years.

A shift in the magnitude of recruits and spawners was also observed through the time series of the SR relationship (Figure 2, color gradient). The aggregated inshore and MA-DMF data sets began in a high-recruitment–high stock size state (green circles; top right of panels) and then clearly transitioned to a low-recruitment–low stock size state by the end of the time series (red circles; bottom left of panels). A similar transition to a low-recruitment–low stock size state occurred in the NMFS-BTS ocean spring, CT-DEEP, and RI-DEM data sets, although these time series began at a relatively lower recruitment but high stock size state. In the NMFS-BTS ocean fall data set, no trend in the time series data was apparent.

DISCUSSION

The effects of spawner abundance, age structure, predation, and temperature were evaluated as drivers of recruitment in SNE/MA Winter Flounder. Dominant drivers of the SR relationship differed across member state data sets and, by association, spatial components of the regional SNE/MA Winter Flounder stock unit. Spatial and behavioral substocks have been identified in SNE/MA Winter Flounder (Ziegler et al. 2018; Siskey et al. 2020), but this work suggests that it is important to consider the drivers

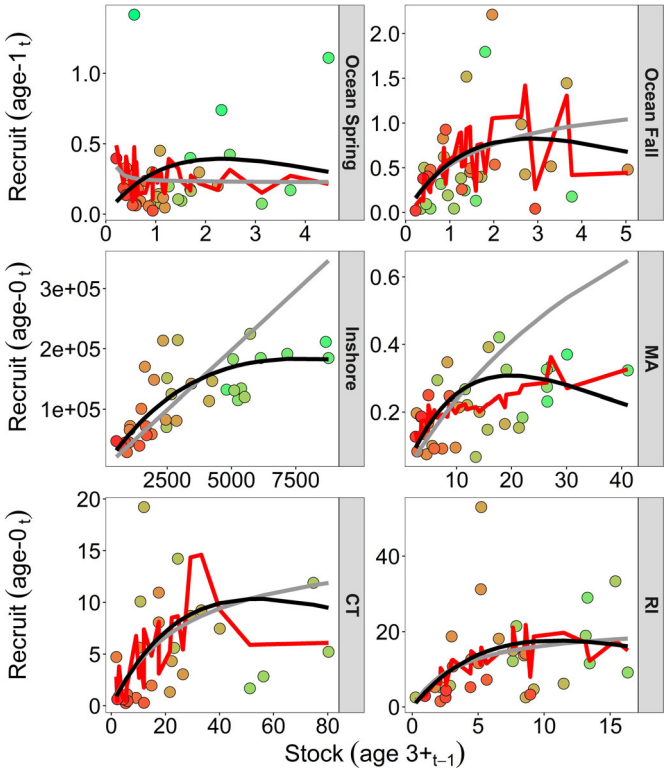

FIGURE 2. Selected top-ranked models (red) for each Winter Flounder data set as determined using Akaike's information criterion, with the base Ricker (black) and Beverton–Holt (gray) models overlain. Units are mean number per tow, except for the aggregated inshore data set, which used a conversion for area swept differences across combined data sets (mean number/km^2). Top-ranked models were as follows: Beverton–Holt with the number of spawner age-classes for Massachusetts (MA), Connecticut (CT), and Rhode Island (RI); Ricker with the number of spawner age-classes for ocean fall; Beverton–Holt with the Summer Flounder predation index for ocean spring; and Ricker for inshore. Circles are respective stock and recruitment data filled with a gradient from green to red across time (~1980–2016).

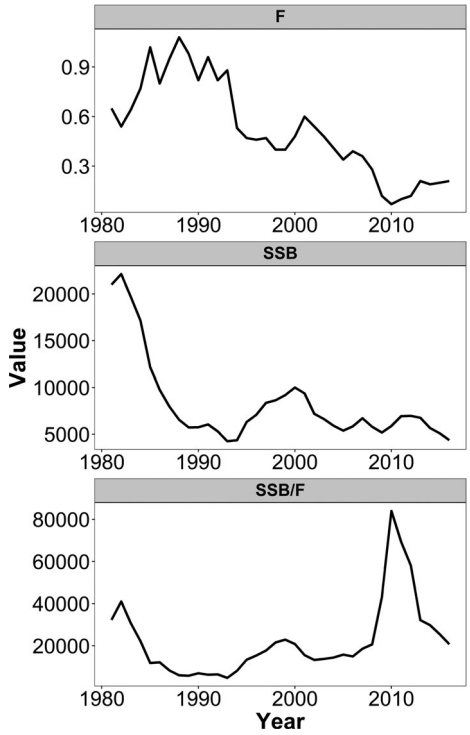

FIGURE 3. Fishing mortality rate (F; top panel) and spawning stock biomass (SSB; middle panel) derived quantities from the 2017 southern New England/mid-Atlantic Winter Flounder stock assessment model over time. The relationship between SSB and F over time is also depicted (bottom panel).

of recruitment for spatial subcomponents of the regional stock unit more formally in terms of explaining uncertainty. Overall, four model comparisons suggested that age structure is a driver of recruitment (i.e., a model including age structure was present in the pool of top-ranked models as determined by ΔAIC). Given the overfished status of this stock and the lack of recovery despite management actions, these findings provide useful information on mechanisms of the SR relationship that are not formally considered in routine stock assessment. For a species that has failed to recover spawner biomass and consistently displays low annual recruitment despite the recent recovery of age structure and reduced fishing effort, long-term fishing reductions (i.e., a moratorium) may be required to promote full recovery.

In 2009, NMFS declared a moratorium for the SNE/MA stock in federal waters; however, the Atlantic States Marine Fisheries Commission allowed commercial and recreational fishing to continue in state waters despite the depletion of the stock (ASMFC 2009). For Winter Flounder, which has a generation time of about 10–15 years, a moratorium of 10–15 years may be necessary for the population to reap the benefits of the rebuilt storage effect, whereby periodic production of strong year-classes by older, larger individuals in years of favorable conditions could spearhead biomass recovery (Secor 2007). This exemplifies the process of hysteresis, in which the way back is often not the same path that was taken forward: in this case, the time to recover biomass in addition to age structure is likely to be considerably longer than the time it took to deplete both of these population attributes (Collie et al. 2004; Secor 2015).

Previous studies analyzing the effect of covariates on the Winter Flounder SR relationship and population projections have primarily focused on integrating the effects of climate change through warming temperatures (Bell et al. 2015, 2018; Frisk et al. 2018); however, a covariate model with temperature only came out as one of the three top-ranked models in the MA-DMF data set and did not emerge as the top-ranked model in any of the comparisons. These previous studies were largely fueled by the

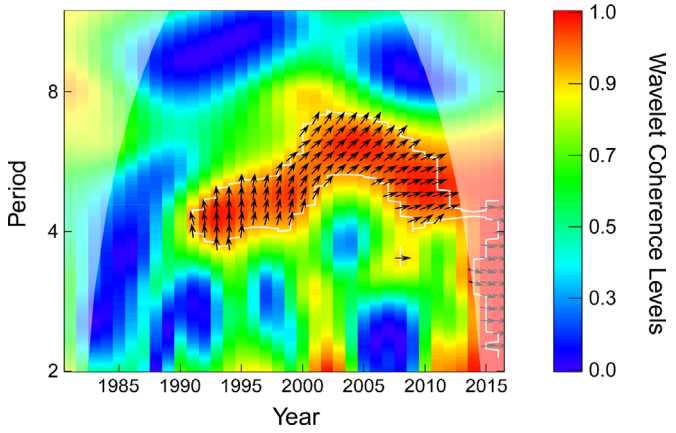

FIGURE 4. Wavelet coherency of the spawning stock biomass time series and the fishing mortality rate time series for Winter Flounder in the time/frequency domain. Red indicates high coherence levels between time series. Lower periods correspond to high-frequency fluctuations, while higher periods correspond to low-frequency fluctuations. Arrows pointing to the right indicate that the two time series are in phase at the respective period with vanishing phase differences, while arrows pointing to the left indicate that the two series are in anti-phase. The white shaded region indicates the cone of influence, where edge effects occur and less credence should be given to significant coherence. The white line delineates areas of significant coherence (red fill).

notion that Winter Flounder, a cold-adapted species, would not flourish under future climate warming scenarios and may already be displaying the negative effects of a climate-altered ecosystem. Although Winter Flounder are likely not unique in how they will respond to climate change compared to other temperate flatfishes, it does appear that overfishing caused the current low-productivity regime (Frisk et al. 2018). However, the impact of climate may be better evaluated through the response of larvae to climate change (Keller and Klein-MacPhee 2000; Rijnsdorp et al. 2009; Pankhurst and Munday 2011) instead of the post-settlement age-0 fish evaluated herein and in previous research.

The Summer Flounder predation index was identified as the most important covariate in one of the data sets (NMFS-BTS ocean spring), suggesting that Summer Flounder abundance may be an important localized driver of Winter Flounder recruitment for the ocean shelf region. Interestingly, the Summer Flounder metric was found to have a moderate negative correlation with the two age structure metrics (−0.49 to −0.66). Age structure metrics declined from about 1980 to 2000, the time period during which Summer Flounder abundance was low and then increased. Thus, it seems that as the age structure of Winter Flounder was in its most depleted state (1995–2000), Summer Flounder abundance was increasing and had a potential effect on recruitment or survival of recruits in the ocean shelf region. Given the positive effects that "big, old, fat, fecund female fish" have on egg size, viability, and the subsequent success of recruitment for those cohorts (Hixon et al. 2014), Winter Flounder recruits may have been hit by large predation events from Summer Flounder at the same time that the quality or quantity of recruits was declining in this system. This could have essentially mimicked an Allee effect (depensation) whereby a decline in the spawning population led to reduced production through low survival of progeny (Myers et al. 1995); however, in previous analyses of Winter Flounder SR dynamics, depensation was not found to be a primary influence for this stock (Frisk et al. 2018).

During the period of declining and depleted age structure (1990–2005), there was significant coherence between F and regional SSB and there was a simultaneous decline in the magnitude of recruits and spawners. Therefore, during the period of high exploitation ($F = 0.8$–1.0; 1985–1995), Winter Flounder age structure and biomass were likely both fished down. In this state, it is common for population abundance and recruitment to become highly variable and to more closely track external forcing (temperature in MA-DMF analyses, Summer Flounder predation in ocean spring analyses; Hsieh et al. 2006; Rouyer et al. 2012). In a reduced demographic state, it is also common for population and recruitment variability to increase due to loss of the stabilizing attributes of the storage effect (Secor 2007).

Our evaluations of covariate times series suggest that the time period of high exploitation and depleted age structure took place during years that were more favorable in terms of predation and BT (positive z-scores; Figure 1), suggesting that these were years with the potential for strong year-class production. However, we suggest that this strong year-class production was not realized due to a depleted age structure and declining spawner abundance. Alternatively, more favorable temperature and predation conditions that occurred during the high-exploitation period (~1980–1995) could have facilitated a delay in our ability to perceive the effects of overexploitation and declining age structure.

Understanding the link between fishing mortality and population dynamics (e.g., SSB and productivity) is fundamental to successful fisheries management. Biological reference points (i.e., biomass target and threshold levels relative to unfished biomass) are often developed to ensure the maintenance of spawning biomass levels that will result in sustainable population renewal. When those reference points are not met, harvest control rules are enacted to reduce fishing effort to a degree where rebuilding can occur. As portrayed through the wavelet analysis, it is evident that the relationship between SSB and F shifted from an out-of-phase state during the period of high fishing pressure and stock collapse (late 1980s and early 1990s) to an in-phase state thereafter. When SSB and F are out of phase, it suggests that reduction of F results in increased

SSB and vice versa—if model output reflects the stock's dynamics. Alternatively, when these metrics are in phase, it suggests that trends track one another and that control of SSB through F may be reduced. In other words, increases in F typically correspond to depletion of SSB and vice versa (i.e., out of phase) when management is effective. If F and SSB are tracking each other through time (i.e., in phase), there may be limited control of population biomass through alterations in fishing. These findings generally match correlations between SSB and F observed by Frisk et al. (2018), where F was (1) significantly and negatively correlated with SSB from 1981 to 1993, (2) negatively correlated with SSB from 1994 to 2000, and (3) positively correlated with SSB from 2001 to 2014. It is possible that the assessment output reflects a real decoupling of F and SSB in the Winter Flounder stock wherein management tools (e.g., catch or effort allocations) would have been ineffective at controlling population biomass during the high-exploitation period had they been in place (e.g., F was not decreased to below the threshold level until 2008; Frisk et al. 2018). However, further research is needed to determine whether the findings of this work are related to model behavior or reflect dynamics of the population.

A limitation of this study was that age structure data were generated from otolith samples taken during the NMFS-BTS, and the information was not expanded to account for the length frequency of the survey catch scaled up by CPUE and stratum area. This means that the age structure data presented herein could be biased so that marginal age-classes (e.g., ages 13–15) are not fully represented. Thus, future work could further develop the age structure data set to incorporate the length frequency data of the survey, which may boost the abundance of older age-classes. However, given the fact that the last few age-classes included in the stock's growth curve all exhibited essentially the same length-bins, it may be difficult to assign ages across the largest length-bins. Nevertheless, use of an age structure data set expanded to the population level could also facilitate hypothesis testing on the effect of reduced and recovering age structure using age-structured stock assessment models within a simulation framework. Additionally, the effects of age structure were not consistent across all models evaluated. Recruitment data are often highly variable, and finding a consistent covariate that explains a significant amount of variation is a challenging task. Research addressing the underlying mechanisms of spawner success and age structure is needed to support field-based metrics of spawners and recruits.

Winter Flounder is not the only groundfish species that has collapsed after persistent overfishing and subsequently failed to recover. The Gulf of Maine stock of Atlantic Cod *Gadus morhua* remains in an overfished state decades since its collapse in the 1990s; however, unlike SNE/MA Winter Flounder, the fishing mortality on this stock remains above threshold levels as of the most recent assessment update (NEFSC 2017b). As a long-depleted, cold-adapted groundfish stock thought to be heading for further depletion in the face of climate change, many recent studies on Winter Flounder have acted as autopsy rather than biopsy; however, we argue that the fate of the SNE/MA Winter Flounder is undecided. The stock is currently not being overfished, and the rebuilding of this stock's age structure over the past decade suggests that stored egg production through the accumulation of older and larger females could result in strong year-class production in future years of favorable environmental conditions (Hixon et al. 2014). Larger, older, and more fecund females are an important component of a spawning population, as they often produce more and larger eggs that are of higher quality and may lead to larvae that grow faster and withstand starvation more readily (Secor 2007; Hixon et al. 2014). Since these large females of iteroparous species contribute disproportionately to reproductive output, they are considered to be the principal contributors to the storage effect purely by outliving years of conditions that are unfavorable for recruitment and continuing to spawn in years of favorable conditions (Barneche et al. 2018). Recruit spawners certainly contribute to the functional diversity of the population, but their contribution is disproportionately less. On the other hand, cryptic population structure may be hiding productive components of the regional stock unit, which are currently considered minor in formal assessment and management frameworks (e.g., bay-resident fish, inshore age-0 recruitment, and ocean recruits; Siskey et al. 2020), suggesting that new stock structure definitions are required.

ACKNOWLEDGMENTS

Research support came from the National Oceanic and Atmospheric Administration's Saltonstall/Kennedy Grant Program (Award Number NA15NMF4270263) and the New York State Department of Environmental Conservation. We thank Robert M. Cerrato for feedback on an earlier version of the manuscript as well as Eric Robillard, Paul Nitschke, and Tony Wood for supplying data and advice. There is no conflict of interest declared in this article.

REFERENCES

Anderson, C. N. K., C. Hsieh, S. A. Sandin, R. Hewitt, A. Hollowed, J. Beddington, R. M. May, and G. Sugihara. 2008. Why fishing magnifies fluctuations in fish abundance. Nature 452:835–839.

ASMFC (Atlantic States Marine Fisheries Commission). 2009. Addendum 1 to the amendment 1 to the interstate fishery management plan for inshore stocks of Winter Flounder. ASMFC, Arlington, Virginia.

Barneche, D. R., D. R. Robertson, C. R. White, and D. J. Marshall. 2018. Fish reproductive-energy output increases disproportionately with body size. Science 360:642–645.

Bell, R. J., D. E. Richardson, J. A. Hare, P. D. Lynch, and P. S. Fratantoni. 2015. Disentangling the effects of climate, abundance, and size on the distribution of marine fish: an example based on four stocks from the northeast US shelf. ICES (International Council for the Exploration of the Sea) Journal of Marine Science 72:1311–1322.

Bell, R. J., A. Wood, J. Hare, D. Richardson, J. Manderson, and T. Miller. 2018. Rebuilding in the face of climate change. Canadian Journal of Fisheries and Aquatic Sciences 75:1405–1414.

Beverton, R. J. H., and S. J. Holt. 1957. On the dynamics of exploited fish populations. Chapman and Hall, London.

Brooks, E. N., and J. J. Deroba. 2015. When "data" are not data: the pitfalls of post hoc analyses that use stock assessment model output. Canadian Journal of Fisheries and Aquatic Sciences 72:634–641.

Burnham, K. P., and D. R. Anderson. 2002. Model selection and multimodel inference: a practical information-theoretic approach, 2nd edition. Springer Verlag, New York.

Cazelles, B. 2008. Wavelet analysis of ecological time series. Oecologia 156:287–304.

Collie, J. S., K. Richardson, and J. H. Steele. 2004. Regime shifts: can ecological theory illuminate the mechanisms? Progress in Oceanography 60:281–302.

DeCelles, G. R., and S. X. Cadrin. 2010. Movement patterns of Winter Flounder (*Pseudopleuronectes americanus*) in the southern Gulf of Maine: observations with the use of passive acoustic telemetry. U.S. National Marine Fisheries Service Fishery Bulletin 108:408–419.

Durant, J. M., M. Hidalgo, T. Rouyer, D. O. Hjermann, L. Ciannelli, A. M. Eikeset, N. Yaragina, and N. C. Stenseth. 2013. Population growth across heterogeneous environments: effects of harvesting and age structure. Marine Ecology Progress Series 480:277–287.

Elmqvist, T., C. Folke, M. Nystrom, G. Peterson, J. Bengtsson, B. Walker, and J. Norberg. 2003. Response diversity, ecosystem change, and resilience. Frontiers in Ecology and the Environment 1:488–494.

Fairchild, E. A. 2017. Indications of offshore spawning by southern Gulf of Maine Winter Flounder. Marine and Coastal Fisheries: Dynamics, Management, and Ecosystem Science [online serial] 9:493–503.

Fairchild, E. A., L. Siceloff, W. H. Howell, B. Hoffman, and M. P. Armstrong. 2013. Coastal spawning by Winter Flounder and a reassessment of essential fish habitat in the Gulf of Maine. Fisheries Research 141:118–129.

Frisk, M. G., T. E. Dolan, A. E. McElroy, J. P. Zacharias, H. Xu, and L. A. Hice. 2018. Assessing the drivers of the collapse of Winter Flounder: implications for management and recovery. Journal of Sea Research 141:1–13.

Harris, P. J., and J. C. McGovern. 1997. Changes in the life history of Red Porgy, *Pagrus pagrus*, from the southeastern United States, 1972–1994. U.S. National Marine Fisheries Service Fishery Bulletin 95:732–747.

Hilborn, R., and C. J. Walters. 1992. Quantitative fisheries stock assessment. Chapman and Hall, New York.

Hixon, M. A., D. W. Johnson, and S. M. Sogard. 2014. BOFFFFs: on the importance of conserving old-growth age structure in fishery populations. ICES (International Council for the Exploration of the Sea) Journal of Marine Science 71:2171–2185.

Hsieh, C., C. S. Reiss, J. R. Hunter, J. R. Beddington, R. M. May, and G. Sugihara. 2006. Fishing elevates variability in the abundance of exploited species. Nature 443:859–862.

Hutchings, J. A. 2000. Collapse and recovery of marine fishes. Nature 406:882–885.

Jeffries, H. P., and W. C. Johnson. 1974. Seasonal distributions of bottom fishes in the Narragansett Bay area: seven-year variations in the abundance of Winter Flounder (*Pseudopleuronectes americanus*). Journal of the Fisheries Research Board of Canada 31:1057–1066.

Jeffries, H. P., and M. Terceiro. 1985. Cycle of changing abundances in the fishes of the Narragansett Bay area. Marine Ecology Progress Series 25:239–244.

Keller, A. A., and G. Klein-MacPhee. 2000. Impact of elevated temperature on the growth, survival, and trophic dynamics of Winter Flounder larvae: a mesocosm study. Canadian Journal of Fisheries and Aquatic Sciences 57:2382–2392.

Kerr, L. A., S. X. Cadrin, D. H. Secor, and N. G. Taylor. 2017. Modeling the implications of stock mixing and life history uncertainty of Atlantic Bluefin Tuna. Canadian Journal of Fisheries and Aquatic Sciences 74:1990–2004.

Manderson, J. P., B. A. Phelan, A. W. Stoner, and J. Hilbert. 2000. Predator–prey relations between age-1+ Summer Flounder (*Paralichthys dentatus*, Linnaeus) and age-0 Winter Flounder (*Pseudopleuronectes americanus*, Walbaum): predator diets, prey selection, and effects of sediments and macrophytes. Journal of Experimental Marine Biology and Ecology 251:17–39.

Myers, R. A., N. J. Barrowman, J. A. Hutchings, and A. A. Rosenberg. 1995. Population dynamics of exploited fish stocks at low population levels. Science 269:1106–1108.

NEFSC (Northeast Fisheries Science Center). 2011. Southern New England/mid-Atlantic Winter Flounder stock assessment. NEFSC, Woods Hole, Massachusetts.

NEFSC (Northeast Fisheries Science Center). 2017a. Southern New England/mid-Atlantic Winter Flounder stock assessment. NEFSC, Woods Hole, Massachusetts.

NEFSC (Northeast Fisheries Science Center). 2017b. Gulf of Maine Atlantic Cod 2017 assessment update report compiled August 2017. NEFSC, Woods Hole, Massachusetts.

NEFSC (Northeast Fisheries Science Center). 2020. State of the ecosystem 2020: mid-Atlantic. NEFSC, Woods Hole, Massachusetts.

Nye, J. A., J. S. Link, J. A. Hare, and W. J. Overholtz. 2009. Changing spatial distribution of fish stocks in relation to climate and population size on the northeast United States continental shelf. Marine Ecology Progress Series 393:111–129.

O'Leary, S. J., L. A. Hice, K. A. Feldheim, M. G. Frisk, A. E. McElroy, M. D. Fast, and D. D. Chapman. 2013. Severe inbreeding and small effective number of breeders in a formerly abundant marine fish. PLOS (Public Library of Science) ONE [online serial] 8(6):e66126.

Pankhurst, N. W., and P. L. Munday. 2011. Effects of climate change on fish reproduction and early life history stages. Marine and Freshwater Research 62:1015–1026.

Perry, R. I., P. Cury, K. Brander, S. Jennings, C. Mollmann, and B. Planque. 2010. Sensitivity of marine systems to climate and fishing: concepts, issues, and management responses. Journal of Marine Systems 79:427–435.

Phelan, B. A. 1992. Winter Flounder movement in the inner New York Bight. Transactions of the American Fisheries Society 121:777–784.

Pinsky, M. L., and M. Fogarty. 2012. Lagged social-ecological responses to climate and range shifts in fisheries. Climate Change 115:883–891.

Planque, B., J. M. Fromentin, P. Cury, K. F. Drinkwater, S. Jennings, R. I. Perry, and S. Kifani. 2010. How does fishing alter marine populations and ecosystems sensitivity to climate? Journal of Marine Systems 79:403–417.

Quinn, T. J., and R. B. Deriso. 1999. Quantitative fish dynamics. Oxford University Press, New York.

R Core Team. 2018. R: a language and environment for statistical computing. R Foundation for Statistical Computing, Vienna.

Ricker, W. E. 1954. Stock and recruitment. Journal of the Fisheries Research Board of Canada 11:559–623.

Rijnsdorp, A. D., M. A. Peck, G. H. Engelhard, C. Mollmann, and J. K. Pinnegar. 2009. Resolving the effect of climate change on fish

populations. ICES (International Council for the Exploration of the Sea) Journal of Marine Science 66:1570–1583.

Roesch, A., and H. Schmidbauer. 2018. WaveletComp: Computational Wavelet Analysis. R package version 1.1. Available: https://CRAN.R-project.org/package=WaveletComp.

Rouyer, T., G. Ottersen, J. M. Durant, M. Hidalgo, D. O. Hjermann, J. Persson, L. C. Stige, and N. C. Stenseth. 2011. Shifting dynamic forces in fish stock fluctuations triggered by age truncation? Global Change Biology 17:3046–3057.

Rouyer, T., S. Sadykov, J. Ohlberger, and N. C. Stenseth. 2012. Does increasing mortality change the response of fish populations to environmental fluctuations? Ecology Letters 15:658–665.

Sagarese, S. R., R. M. Cerrato, and M. G. Frisk. 2011. Diet composition and feeding habits of common fishes in Long Island bays, New York. Northeastern Naturalist 18:291–314.

Sagarese, S. R., and M. G. Frisk. 2011. Movement patterns and residence of adult Winter Flounder within a Long Island estuary. Marine and Coastal Fisheries: Dynamics, Management, and Ecosystem Science [online serial] 3:295–306.

Secor, D. H. 2007. The year-class phenomenon and the storage effect in marine fishes. Journal of Sea Research 57:91–103.

Secor, D. H. 2015. Migration ecology of marine fishes. Johns Hopkins University Press, Baltimore, Maryland.

Siskey, M. R., M. G. Frisk, R. M. Cerrato, and K. E. Limburg. 2020. Redefining spatial population structure of Winter Flounder (*Pseudopleuronectes americanus*): implications for stock assessment and management. Canadian Journal of Fisheries and Aquatic Sciences 77:1189–1200.

Siskey, M. R., M. J. Wilberg, R. J. Allman, B. K. Barnett, and D. H. Secor. 2016. Forty years of fishing: changes in age structure and stock mixing in northwestern Atlantic Bluefin Tuna (*Thunnus thynnus*) associated with size-selective and long-term exploitation. ICES (International Council for the Exploration of the Sea) Journal of Marine Science 73:2518–2528.

Taylor, D. L., and J. S. Collie. 2003. Effect of temperature on the functional response and foraging behavior of the sand shrimp *Crangon septemspinosa* preying on juvenile Winter Flounder *Pseudopleuronectes americanus*. Marine Ecology Progress Series 263:217–234.

Vert-pre, K. A., R. O. Amoroso, O. P. Jensen, and R. Hilborn. 2013. Frequency and intensity of productivity regime shifts in marine fish stocks. Proceedings of the National Academy of Sciences of the United States of America 110:1779–1784.

Wuenschel, M. J., K. W. Able, and D. Byrne. 2009. Seasonal patterns of Winter Flounder *Pseudopleuronectes americanus* abundance and reproductive condition on the New York Bight continental shelf. Journal of Fish Biology 74:1508–1524.

Ziegler, C. M., J. P. Zacharias, and M. G. Frisk. 2018. Migration diversity, spawning behavior, and habitat utilization of Winter Flounder. Canadian Journal of Fisheries and Aquatic Sciences 76:1503–1514.

Appendix: Relationships between Predicted and Observed Recruitment

TABLE A.1. Slope and adjusted r^2 values for the relationship between predicted and observed recruitment of Winter Flounder for the top-five ranked models (BH = Beverton–Holt; ACs = number of spawner age-classes; RS = percent recruit spawners; BT = bottom temperature; SF = Summer Flounder predation index). The models reported for each area are ordered based on ranking. Agency (area) acronyms are defined in Table 1. The slopes and r^2 values reported here correspond to the blue lines in Figure A.1.

Area	Model	Slope	Adjusted r^2
NMFS-BTS ocean spring	SF BH	0.128	0.113
	BT BH	0.112	0.164
	RS BH	0.038	−0.004
	BH	0.001	−0.028
	ACs BH	0.012	−0.023
NMFS-BTS ocean fall	ACs Ricker	0.311	0.193
	ACs BH	0.316	0.185
	SF Ricker	0.214	0.131
	SF BH	0.208	0.102
	Ricker	0.141	0.109
Inshore	Ricker	0.603	0.529
	BH	1.066	0.485
	ACs BH	−1.497	0.049
	SF BH	3.813	0.307
	BT BH	9.208	0.472
MA-DMF	ACs BH	0.34	0.307
	BT BH	0.352	0.339
	RS BH	0.305	0.284
	SF BH	0.297	0.313
	BT Ricker	0.419	0.332
CT-DEEP	ACs BH	0.419	0.284
	SF Ricker	0.435	0.267
	ACs Ricker	0.474	0.246
	SF BH	0.377	0.156
	RS BH	0.461	0.272
RI-DEM	ACs BH	0.169	0.115
	BH	0.137	0.113
	ACs Ricker	0.18	0.104
	Ricker	0.148	0.106
	RS BH	0.14	0.09

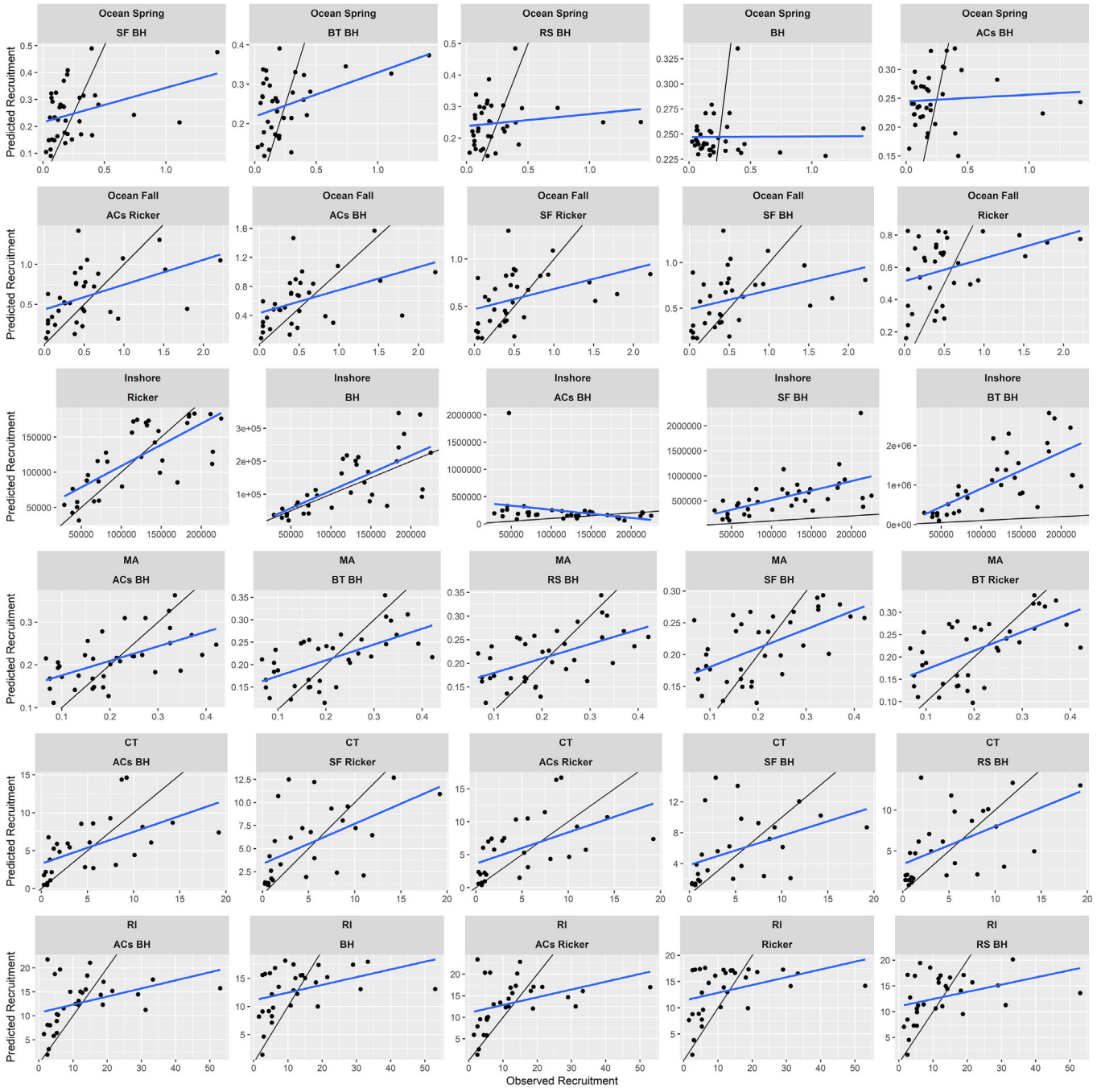

FIGURE A.1. The relationship between predicted and observed recruitment of Winter Flounder for the top-five ranked models for each data set. Panels are ordered from left to right by ranking. Models are defined in Table A.1. Slopes and r^2 values for the blue lines are reported in Table A.1. Units of recruitment were mean numbers-per-tow for all data sets except for the Inshore data set. For the Inshore data set, the stock and recruitment indices of abundance from state surveys were separately expanded for area swept, summed across age-classes, and then aggregated by averaging across state surveys (mean numbers/km^2). Recruitment refers to age-1 individuals for the Ocean Fall and Ocean Spring datasets, and age-0 individuals for all other datasets.

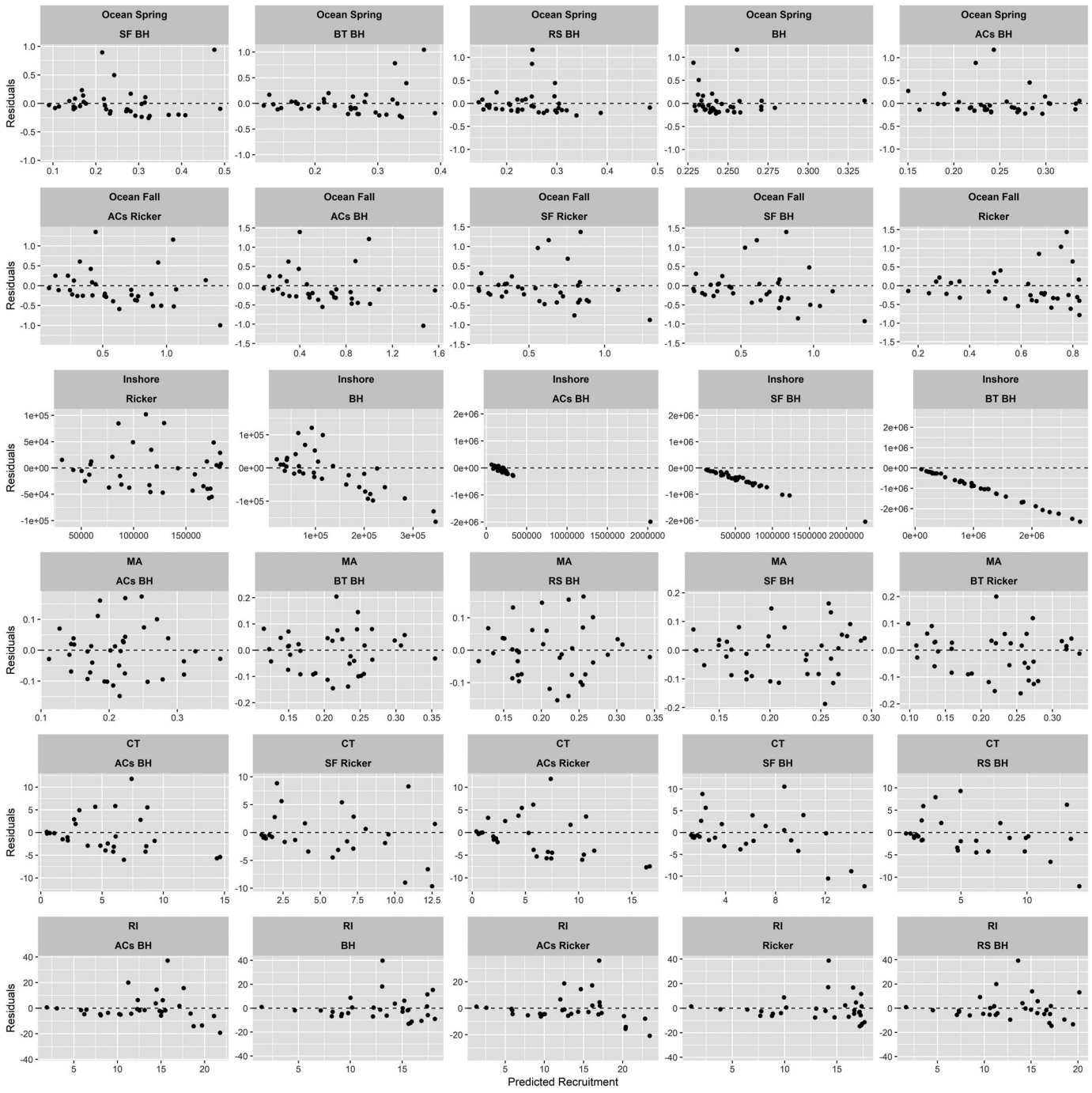

FIGURE A.2. The relationship between residuals (observed − predicted recruitment) and predicted recruitment of Winter Flounder for the top-five ranked models from each data set. Panels are ordered from left to right by ranking. Models are defined in Table A.1.